

Fairness with Continuous Optimal Transport

Silvia Chiappa,^{1*} Aldo Pacchiano^{2*}

¹DeepMind, ²UC Berkeley
csilvia@google.com, pacchiano@berkeley.edu

Abstract

Whilst optimal transport (OT) is increasingly being recognized as a powerful and flexible approach for dealing with fairness issues, current OT fairness methods are confined to the use of discrete OT. In this paper, we leverage recent advances from the OT literature to introduce a stochastic-gradient fairness method based on a dual formulation of continuous OT. We show that this method gives superior performance to discrete OT methods when little data is available to solve the OT problem, and similar performance otherwise. We also show that both continuous and discrete OT methods are able to continually adjust the model parameters to adapt to different levels of unfairness that might occur in real-world applications of ML systems.

Introduction

ML fairness techniques aim at ensuring that models do not encode nor amplify human and societal biases contained in the training data, and therefore that individuals are not treated unfavorably on the basis of race, gender, disabilities, or other *sensitive attributes* (Gajane and Pechenizkiy 2017; Mitchell, Potash, and Barocas 2018; Verma and Rubin 2018; Barocas, Hardt, and Narayanan 2019; Oneto and Chiappa 2020).

Popular fairness criteria such as *demographic parity* require certain characteristics of relevant distributions to be invariant to different sensitive attributes. Whilst facilitating model evaluation and design, in many real-world scenarios invariance of the entire distributions might instead be necessary to ensure fairness.

Optimal transport (OT) (Villani 2009; Peyré 2019) is increasingly being explored to impose statistical independence *w.r.t.* sensitive attributes through enforcing small OT distances between distributions, allowing to achieve a stronger version of demographic parity as well as other criteria (Black, S., and Fredrikson 2019; Del Barrio et al. 2019; Johndrow and Lum 2019; Risser et al. 2019; Wang, Ustun, and Calmon 2019; Chzhen et al. 2020; Del Barrio, Gordaliza, and Loubes 2020; Le Gouic and Loubes 2020; Yurochkin, Bower, and Sun 2020).

As observed in Jiang et al. (2019); Chiappa et al. (2020), OT distances can explicitly be related to expected changes

in model accuracy. This makes the application of OT to fairness particularly attractive, as it allows to devise methods for achieving statistical independence with minimal loss of accuracy and therefore with optimal fairness-accuracy trade-offs.

Current methods approximate the computation of OT distances between continuous distributions with discrete OT. Building on the recent advances in avoiding such approximations (Genevay et al. 2016; Genevay 2019; Mensch and Peyré 2020), we introduce a stochastic-gradient fairness method based on a dual formulation of continuous OT. We show that this method gives superior performance to discrete OT methods when little data is available to solve the OT problem, and similar performance otherwise. In addition, we show that OT methods are able to continually adjust the model parameters to adapt to changes in level of unfairness, and therefore demonstrate their suitability in real-world applications in which the data used for system training and deployment differ in unfairness levels.

Related Work

Recent literature on fairness has seen an increase in the adoption of OT. Our approach is close to the penalty approach proposed in Jiang et al. (2019), and differs from it in using continuous, rather than discrete, OT. Whilst detailed and evaluated on classification and on *strong demographic parity*, in a similar way as done in Chiappa et al. (2020) our method can be modified to solve regression problems and to achieve other fairness criteria, including strong equalized odds and causal criteria such as (path-specific) counterfactual fairness. Unlike our method, other in-processing methods to achieve strong demographic parity such as adversarial ones focus on binary sensitive attributes (Zhang, Lemoine, and Mitchell 2018; Celis and Vijay Keswani 2019).

The adjustment capabilities to changing levels of unfairness that we show in this paper can be placed within the broader context of recent efforts in the ML fairness literature to go beyond the static fairness assumption. However, these capabilities are complementary to those of approaches accounting for downstream impact of decisions (Joseph et al. 2016; Jabbari et al. 2017; Blum et al. 2018; Gillen et al. 2018; Liu et al. 2018; Creager et al. 2019; Sun et al. 2019; Tabibian et al. 2019; Wen, Bastani, and Topcu 2019; Zhang and Liu 2020). These latter approaches aim at prospectively

*Equal contribution.

addressing long-term effects that induce changes in unfairness levels during the training of the model. We instead aim at retrospectively modify the model parameters to account for different unfairness levels. Such differences could be due to downstream impact of decisions or to other, social, factors, *e.g.*, for the case of a risk assessment instruments, to differing rates of policing in neighborhoods that are more disproportionately populated by non-Whites (Lum and Isaac 2016; Rosenberg and Levinson 2018). These adjustment capabilities are also different from robustness to changes in the data distribution enforced during training of the model (Mandal et al. 2020).

SDP-Fair Classification with OT

We focus on the problem of enforcing strong demographic parity (SDP) in binary classification.

Consider the problem of learning a binary classification model from a dataset $\mathcal{D} = \{(a^n, x^n, y^n)\}_{n=1}^N$ —with underlying joint distribution $p(A, X, Y)$ —corresponding to N individuals, in which $x^n \in \mathbb{R}^d$ is a vector of features, $a^n \in \mathcal{A} = \mathbb{N}^k$ is a vector of attributes that are considered sensitives, and y^n is a binary class label.

We assume that the model output for individual n , s^n , represents an estimate of the probability of belonging to class 1, $p(Y = 1|A = a^n, X = x^n)$. A prediction \hat{y}^n of y^n is then obtained as $\hat{y}^n = \mathbb{1}_{s^n > \tau}$, where $\mathbb{1}_{s^n > \tau} = 1$ if $s^n > \tau$ for a threshold $\tau \in [0, 1]$ and zero otherwise. The model outputs induce a random variable S . We indicate with p_S the distribution of S and with p_{S_a} the conditional distribution of S given sensitive attributes a .

SDP requires statistical independence between S and A , and can be expressed as

$$\text{SDP: } p_{S_a} = p_{S_{\bar{a}}}, \forall a, \bar{a} \in \mathcal{A}.$$

Over demographic parity ($\langle \hat{Y} \rangle_{p(\hat{Y}|A=a)} = \langle \hat{Y} \rangle_{p(\hat{Y}|A=\bar{a})}$), SDP has the advantage of ensuring that the class predictions do not depend on the sensitive attributes regardless of the value of the threshold τ used. SDP is also desirable if scores rather than binary predictions are the target outcomes—such as *e.g.* in risk assessment instruments where scores represent risk of re-committing a crime—as SDP would ensure that the scores do not depend on the sensitive attributes.

Our approach to impose SDP follows closely the penalty approach introduced in Jiang et al. (2019). After training the model using a standard loss, we modify the obtained model parameters to minimize the OT distances between the groups distributions $\{p_{S_a}\}$ and a target distribution $p_{\bar{S}}$. However, we propose a method that does not require approximating such distances with discrete OT. Whilst any target distribution $p_{\bar{S}}$ and type of OT distance would allow to achieve SDP, for classification using the barycenter of $\{p_{S_a}\}$ and the Wasserstein-1 distance ensures optimal fairness-accuracy trade-offs (see Jiang et al. (2019)).

Computation of OT Distances

As part of a recent effort toward providing solutions for the computation of OT distances between continuous distributions, Genevay et al. (2016); Genevay (2019) introduced a

stochastic-gradient method for solving an entropy regularized continuous OT problem using samples from the distributions. We propose to compute OT distances between $\{p_{S_a}\}$ and $p_{\bar{S}}$ by adapting this method to our setting.

Background on Continuous OT

Let p_X and p_Y be two probability density functions (pdfs) on \mathcal{X} and \mathcal{Y} , $\Gamma(p_X, p_Y)$ the set of joint pdfs on $\mathcal{X} \times \mathcal{Y}$ with marginals p_X and p_Y , and $\mathcal{C} : \mathcal{X} \times \mathcal{Y} \rightarrow [0, \infty]$ a *cost function*.

The Kantorovich OT problem (Kantorovich 1942; Villani 2009; Peyré 2019) consists in finding a $\gamma^* \in \Gamma(p_X, p_Y)$, called the *optimal coupling* between p_X and p_Y , minimizing the expected cost with respect to $\gamma(x, y)$, *i.e.* such that

$$\gamma^* = \arg \min_{\gamma \in \Gamma(p_X, p_Y)} \langle \mathcal{C}(x, y) \rangle_{\gamma(x, y)}, \quad (1)$$

where $\langle \mathcal{C}(x, y) \rangle_{\gamma(x, y)} := \int_{\mathcal{X} \times \mathcal{Y}} \mathcal{C}(x, y) \gamma(x, y) dx dy$. Under appropriate conditions on \mathcal{C} ,

$$\mathcal{W}_{\mathcal{C}}(p_X, p_Y) := \min_{\gamma \in \Gamma(p_X, p_Y)} \langle \mathcal{C}(x, y) \rangle_{\gamma(x, y)}$$

is a distance between p_X and p_Y , called *OT distance*.

Our setting ($S \in [0, 1]$) gives $\mathcal{X} = \mathcal{Y} = [0, 1]$, and we consider $\mathcal{C}(x, y) = \|x - y\|_1$, where $\|\cdot\|_1$ indicates the L^1 -norm. The resulting OT distance, that we denote with the shorthand $\mathcal{W}_1(p_X, p_Y)$, is known as the *Wasserstein-1 distance*.

Dual Formulation of Regularized Continuous OT

Problem (1) has dual formulation given by

$$\begin{aligned} \lambda_X^*, \lambda_Y^* = \arg \max_{\lambda_X \in \mathcal{C}(\mathcal{X}), \lambda_Y \in \mathcal{C}(\mathcal{Y})} & \langle \lambda_X(x) \rangle_{p_X(x)} + \langle \lambda_Y(y) \rangle_{p_Y(y)} \\ \text{s.t. } & \lambda_X(x) + \lambda_Y(y) \leq \mathcal{C}(x, y) \quad \forall x, y, \end{aligned} \quad (2)$$

where $\mathcal{C}(\cdot)$ indicates the space of continuous functions. The dual formulation has the advantage of containing expectations *w.r.t.* the marginals p_X and p_Y , which can be estimated using samples from these distributions. However, due to the difficulty in fulfilling the constraint $\lambda_X(x) + \lambda_Y(y) \leq \mathcal{C}(x, y)$, Genevay et al. (2016); Genevay (2019) suggest to consider a regularized version of Problem (1) given by

$$\gamma^* = \arg \min_{\gamma \in \Gamma(p_X, p_Y)} \langle \mathcal{C}(x, y) \rangle_{\gamma(x, y)} + \lambda \mathcal{D}_{\phi}[\gamma|p_X p_Y], \quad (3)$$

where $\mathcal{D}_{\phi}[\gamma|p_X p_Y] := \left\langle \phi\left(\frac{\gamma(x, y)}{p_X(x)p_Y(y)}\right) \right\rangle_{p_X(x)p_Y(y)}$ is the ϕ -divergence between γ and $p_X p_Y$ (Csiszar 1975), and λ is a scalar that controls the regularization strength. We indicate the regularized OT distance with $\mathcal{W}_{\mathcal{C}}^{\lambda}(p_X, p_Y)$.

Following Genevay et al. (2016); Seguy et al. (2018); Genevay (2019); Lee, Pacchiano, and Jordan (2020), we consider¹ $\phi(x) = x \log(x) - x$, obtaining the *relative entropy regularization*

$$\mathcal{D}_{\phi}[\gamma|p_X p_Y] = \left\langle \log\left(\frac{\gamma(x, y)}{p_X(x)p_Y(y)}\right) - 1 \right\rangle_{\gamma(x, y)},$$

¹We consider $\phi(x) = x \log(x) - x$ rather than $\phi(x) = x \log(x)$, as this leads to a simpler formulation.

and $\phi(x) = x^2 + i_{\mathbb{R}^+}(x)$, where i denotes the convex indicator function, obtaining the L^2 regularization

$$\mathcal{D}_\phi[\gamma|p_X p_Y] = \left\langle \left(\frac{\gamma(x, y)}{p_X(x)p_Y(y)} \right)^2 \right\rangle_{p_X(x)p_Y(y)}.$$

Problem (3) has dual formulation given by

$$\lambda_X^*, \lambda_Y^* = \arg \max_{\lambda_X \in \mathcal{C}(\mathcal{X}), \lambda_Y \in \mathcal{C}(\mathcal{Y})} \left\langle \lambda_X(x) + \lambda_Y(y) - \lambda \phi^* \left(\frac{\lambda_X(x) + \lambda_Y(y) - \mathcal{C}(x, y)}{\lambda} \right) \right\rangle_{p_X(x)p_Y(y)}, \quad (4)$$

where $\phi^*(x) = \exp(x)$ for the relative entropy regularization, and $\phi^*(x) = \max(x, 0)^2/4$ for the L^2 regularization.

Proof. Indicating with λ_X and λ_Y the Lagrange multipliers, we can write the dual function as

$$\begin{aligned} & \min_{\gamma(x, y)} \langle \mathcal{C}(x, y) \rangle_{\gamma(x, y)} + \lambda \left\langle \phi \left(\frac{\gamma(x, y)}{p_X(x)p_Y(y)} \right) \right\rangle_{p_X(x)p_Y(y)} \\ & + \left\langle p_X(x) - \int_Y \gamma(x, y) dy \right\rangle_{\lambda_X(x)} + \left\langle p_Y(y) - \int_X \gamma(x, y) dx \right\rangle_{\lambda_Y(y)} \\ & = \langle \lambda_X(x) \rangle_{p_X(x)} + \langle \lambda_Y(y) \rangle_{p_Y(y)} + \lambda \min_{\gamma(x, y)} \left\langle \phi \left(\frac{\gamma(x, y)}{p_X(x)p_Y(y)} \right) - \frac{\lambda_X(x) + \lambda_Y(y) - \mathcal{C}(x, y)}{\lambda} \right\rangle_{p_X(x)p_Y(y)} \\ & = \left\langle \lambda_X(x) + \lambda_Y(y) - \lambda \phi^* \left(\frac{\lambda_X(x) + \lambda_Y(y) - \mathcal{C}(x, y)}{\lambda} \right) \right\rangle_{p_X(x)p_Y(y)}, \end{aligned}$$

where ϕ^* is the Legendre transform of ϕ , i.e. $\phi^*(x^*) := \max_x (x^*x - \phi(x))$. \square

Dual Variables Parametrization

Following Genevay et al. (2016); Genevay (2019), we parametrize the *dual variables* λ_X and λ_Y as expansions in reproducing kernel Hilbert spaces using the random Fourier features approximation introduced in Rahimi and Recht (2008). More specifically, we approximate a Gaussian kernel κ with variance σ^2 as

$$\kappa(x, x') \approx \frac{2}{D} \sum_{i=1}^D \cos(\omega^i x + b^i) \cos(\omega^i x' + b^i),$$

where $\omega^i \sim \mathcal{N}(0, 2/\sigma^2)$ and $b^i \sim U[0, 2\pi]$, with $\mathcal{N}(\cdot, \cdot)$ and $U[\cdot, \cdot]$ indicating the Gaussian and uniform distributions respectively. This way we can express $\lambda_X(x)$ as

$$\lambda_X(x) \approx \lambda_X^\top \psi_{\lambda_X}(x),$$

where λ_X is a D -dimensional vector² and

$$\psi_{\lambda_X}(x) = \sqrt{\frac{2}{D}} (\cos(\omega^1 x + b^1), \dots, \cos(\omega^D x + b^D))^\top.$$

²Throughout the paper, we use an abuse of notation by overloading the symbol λ_X to denote both a function and a vector. The meaning should be clear from the context.

It is possible to show that, if $D = \tilde{\mathcal{O}}(1/\epsilon^2)$, the random feature maps can achieve an approximation error of ϵ w.r.t. the original Gaussian kernel (see Claim 1 in Rahimi and Recht (2008)). Experimentally, we did not see significant difference in performance for $D \geq 50$.

Optimal Dual Variables

Using samples $\{x^i\}_{i=1}^{N_x}$ and $\{y^j\}_{j=1}^{N_y}$ from p_X and p_Y , we can form a Monte-Carlo approximation of the expectation in Problem (4), and find the optimal dual variables through stochastic gradient. Specifically, the gradient with respect to λ_X is given by

$$\begin{aligned} \nabla_{\lambda_X} & \left(\frac{1}{N_x} \sum_{i=1}^{N_x} \lambda_X(x^i) + \frac{1}{N_y} \sum_{j=1}^{N_y} \lambda_Y(y^j) - \frac{\lambda}{N_x N_y} \sum_{i=1}^{N_x} \sum_{j=1}^{N_y} \phi^* \left(\frac{\lambda_X(x^i) + \lambda_Y(y^j) - \mathcal{C}(x^i, y^j)}{\lambda} \right) \right) \\ & = \frac{1}{N_x} \sum_{i=1}^{N_x} \left(1 - \frac{\lambda}{N_y} \sum_{j=1}^{N_y} \phi^*(x^i, y^j)' \right) \psi_{\lambda_X}(x^i), \end{aligned}$$

where $\phi^*(x^i, y^j)' = \frac{1}{\lambda} \exp\left(\frac{\lambda_X(x^i) + \lambda_Y(y^j) - \mathcal{C}(x^i, y^j)}{\lambda}\right)$ for the relative entropy regularization, whilst $\phi^*(x^i, y^j)' = \frac{1}{2\lambda^2} (\lambda_X(x^i) + \lambda_Y(y^j) - \mathcal{C}(x^i, y^j))$ for the L^2 regularization. This suggests the following stochastic-gradient update

$$\lambda_X \leftarrow \lambda_X + \frac{\epsilon \lambda}{N_x} \sum_{i=1}^{N_x} \left(1 - \frac{1}{N_y} \sum_{j=1}^{N_y} \alpha_{ij} \right) \psi_{\lambda_X}(x^i), \quad (5)$$

where ϵ_λ is the update size and $\alpha_{ij} := \lambda \phi^*(x^i, y^j)'$.

Enforcing $\lambda_X(x) + \lambda_Y(x) = 0$. In the limit $\lambda \rightarrow 0$, for a cost function satisfying $\mathcal{C}(x, x) = 0 \forall x$, the soft constraint given by $-\lambda \phi^*\left(\frac{\lambda_X(x) + \lambda_Y(y) - \mathcal{C}(x, y)}{\lambda}\right)$ in Problem (4) converges to the hard constraint of Problem (2). Whenever the hard constraint is enforced, $\lambda_X(x) + \lambda_Y(x) \leq 0 \forall x$, and therefore $\lambda_Y(x) = -\lambda_X(x) - \xi(x)$ for some non-negative function ξ , giving

$$\begin{aligned} & \langle \lambda_X(x) \rangle_{p_X(x)} + \langle \lambda_Y(y) \rangle_{p_Y(y)} \\ & = \langle \lambda_X(x) \rangle_{p_X(x)} - \langle \lambda_X(y) \rangle_{p_Y(y)} - \langle \xi(y) \rangle_{p_Y(y)} \\ & \leq \langle \lambda_X(x) \rangle_{p_X(x)} - \langle \lambda_X(y) \rangle_{p_Y(y)}. \end{aligned}$$

If λ_X and $-\lambda_X$ also satisfy the constraint of Problem (2), the duple $(\lambda_X, -\lambda_X)$ is a better candidate to achieve the optimum of Problem (2), suggesting that we can restrict the optimization to (λ_X, λ_Y) satisfying

$$\lambda_X(x) + \lambda_Y(x) = 0.$$

This argument is used for example when $\mathcal{C}(x, y) = \|x\|_1$ and λ_X, λ_Y are constrained to be 1-Lipschitz (Arjovsky, Chintala, and Bottou 2017). We use this strategy to stabilize

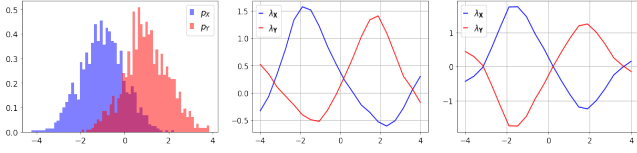


Figure 1: **Left:** Histograms of two Gaussians $\mathcal{N}(-1, 1)$ and $\mathcal{N}(1, 1)$. **Center:** Optimal dual variables obtained using the stochastic-gradient method described above. **Right:** Optimal dual variables with constraint $\lambda_X(x) + \lambda_Y(x) = 0$.

the optimization problem. With this constraint, update (5) needs to be adjusted by adding to it the term

$$-\frac{\epsilon\lambda}{N_y} \sum_{j=1}^{N_y} \left(1 - \frac{1}{N_x} \sum_{i=1}^{N_x} \alpha_{ij}\right) \psi_{\lambda_X}(y^j).$$

Intuition on Dual Variables. If we disregard the last term in Problem (4), we obtain $\mathcal{W}_C^\lambda(p_X, p_Y) \approx \langle \lambda_X^*(x) \rangle_{p_X(x)} + \langle \lambda_Y^*(y) \rangle_{p_Y(y)}$. This indicates that the optimal dual variable λ_X^* achieves large values in regions of the support where p_X differs the most from p_Y and vice-versa, as illustrated in Fig. 1 for two Gaussian distributions with differing means.

COT Method

In this section, we introduce a stochastic-gradient method that modifies the parameters of a binary classifier in order to achieve SDP using the approach for computing OT distances described above.

We assume that the model output s^n is obtained with the logistic function, *i.e.*

$$s^n = g_\theta(a^n, x^n) := 1 / (1 + \exp(-\theta^\top(a^n, x^n)^\top)),$$

where $\theta \in \mathbb{R}^{k+d}$ are the model parameters. After training the model using the standard logistic regression loss, we modify the obtained θ^* to minimize the sum over $a \in \mathcal{A}$ of the regularized Wasserstein-1 distances between p_{S_a} (which depends on θ) and a target distribution $p_{\bar{S}}$ (which we keep fixed at θ^*), *i.e.* to solve the following problem

$$\min_{\theta} \sum_{a \in \mathcal{A}} \mathcal{W}_1^\lambda(p_{S_a}, p_{\bar{S}}). \quad (6)$$

Indicating with λ_{S_a} and $\lambda_{\bar{S},a}$ the dual variables associated to $\mathcal{W}_1^\lambda(p_{S_a}, p_{\bar{S}})$, the dual formulation of Problem (6) can be expressed as

$$\min_{\theta} \sum_{a \in \mathcal{A}} \max_{\lambda_{S_a}, \lambda_{\bar{S},a}} \left(\langle \lambda_{S_a}(s) \rangle_{p_{S_a}(s)} + \langle \lambda_{\bar{S},a}(\bar{s}) \rangle_{p_{\bar{S}}(\bar{s})} - \left\langle \lambda \phi^* \left(\frac{\lambda_{S_a}(s) + \lambda_{\bar{S},a}(\bar{s}) - \mathcal{C}(s, \bar{s})}{\lambda} \right) \right\rangle_{p_{S_a}(s) p_{\bar{S}}(\bar{s})} \right). \quad (7)$$

We propose to solve Problem (7) with a stochastic-gradient approach that alternates between the following two steps:

1. Perform a gradient update of the dual variables λ_{S_a} and $\lambda_{\bar{S},a}$, $\forall a \in \mathcal{A}$, keeping the model parameters θ fixed.

COT Algorithm

Input: Regularization strength λ . Number of random Fourier features D . Kernel variance σ^2 . Dual variables and parameters update sizes $\epsilon_\lambda, \epsilon_\theta$. Number of updates K . Batch sizes $N_S, N_{\bar{S}}$.

Learn θ^* with standard logistic regression. Set $\theta = \theta^*$.

Create dataset $\bar{\mathcal{D}}$ representing $p_{\bar{S}}$.

Initialize dual variables as $\lambda_{S_a} = \mathbf{0}, \lambda_{\bar{S},a} = \mathbf{0}, \forall a \in \mathcal{A}$.

for $k = 1, \dots, K$ **do**

 Sample $\{\bar{s}_t^j\}_{j=1}^{N_{\bar{S}}}$ from $\bar{\mathcal{D}}$.

for $a \in \mathcal{A}$ **do**

 Sample $\{(a^i = a, x^i, y^i)\}_{i=1}^{N_S}$ from \mathcal{D} and create the model outputs $\{s_a^i = g_\theta(a, x^i)\}_{i=1}^{N_S}$.

 Compute $\alpha_{ij} = \lambda \phi^*(s_a^i, \bar{s}^j)'$.

 Update dual variables

$$\lambda_{S_a} \leftarrow \lambda_{S_a} + \frac{\epsilon_\lambda}{N_{S_a}} \sum_{i=1}^{N_S} \left(1 - \frac{\sum_{j=1}^{N_{\bar{S}}} \alpha_{ij}}{N_{\bar{S}}}\right) \psi_{\lambda_{S_a}}(s_a^i),$$

$$\lambda_{\bar{S},a} \leftarrow \lambda_{\bar{S},a} + \frac{\epsilon_\lambda}{N_{\bar{S}}} \sum_{j=1}^{N_{\bar{S}}} \left(1 - \frac{\sum_{i=1}^{N_S} \alpha_{ij}}{N_S}\right) \psi_{\lambda_{\bar{S},a}}(\bar{s}^j).$$

 Update parameters

$$\theta \leftarrow \theta - \epsilon_\theta \sum_{a \in \mathcal{A}} \sum_{i=1}^{N_S} \sum_{j=1}^{N_{\bar{S}}} \left((1 - \alpha_{ij}) \nabla_{g_\theta} \lambda_{S_a}(s_a^i) + \alpha_{ij} \nabla_{g_\theta} \mathcal{C}(s_a^i, \bar{s}^j) \right) \nabla_{\theta} s_a^i.$$

Return: $\theta; \lambda_{S_a}, \lambda_{\bar{S},a} \forall a \in \mathcal{A}$.

2. Perform a gradient update of the model parameters θ , keeping the dual variables λ_{S_a} and $\lambda_{\bar{S},a}$ fixed.

The steps are achieved with samples $\{(a^i = a, x^i, y^i)\}_{i=1}^{N_S} \forall a \in \mathcal{A}$ from the training dataset \mathcal{D} , which are used to create the model outputs $\{s_a^i = g_\theta(a, x^i)\}_{i=1}^{N_S}$, and with samples $\{\bar{s}^j\}_{j=1}^{N_{\bar{S}}}$ from a dataset $\bar{\mathcal{D}}$ representing the target distribution $p_{\bar{S}}$, and have computational cost $\mathcal{O}(N_S(N_{\bar{S}} + D))$. The gradient updates are explained in detail below. The full procedure is summarized in the COT Algorithm above.

1. Dual Variables Update. Using the explanation above, in the unconstrained case the updates for the dual variables are obtained as

$$\lambda_{S_a} \leftarrow \lambda_{S_a} + \frac{\epsilon_\lambda}{N_{S_a}} \sum_{i=1}^{N_S} \left(1 - \frac{1}{N_{\bar{S}}} \sum_{j=1}^{N_{\bar{S}}} \alpha_{ij}\right) \psi_{\lambda_{S_a}}(s_a^i),$$

$$\lambda_{\bar{S},a} \leftarrow \lambda_{\bar{S},a} + \frac{\epsilon_\lambda}{N_{\bar{S}}} \sum_{j=1}^{N_{\bar{S}}} \left(1 - \frac{1}{N_S} \sum_{i=1}^{N_S} \alpha_{ij}\right) \psi_{\lambda_{\bar{S},a}}(\bar{s}^j).$$

2. Model Parameters Update. The first and third expectations in Problem (7) are *w.r.t.* the model outputs distribution p_{S_a} which (unlike $p_{\bar{S}}$) is a function of θ , making the minimization *w.r.t.* θ a challenging task. This difficulty can be

	Adult				German Credit				Community & Crime			
	Err-.5	Wass1	SDD	SPDD	Err-.5	Wass1	SDD	SPDD	Err-.5	Wass1	SDD	SPDD
LR	.142	.313	.426	.806	.248	.103	.102	.102	.116	1.435	1.402	7.649
DOT	.175	.027	.023	.054	.282	.035	.020	.020	.327	.207	.176	.848
DPP	.170	.025	.017	.043	.248	.032	.024	.024	.327	.356	.159	.821
COT	.175	.023	.020	.044	.242	.042	.027	.027	.324	.223	.204	.928

Table 1: Test classification error (Err-.5) and unfairness level (Wass1, SDD, and SPDD) for logistic regression (LR), the methods in Jiang et al. (2019) (DOT and DPP), and COT on the UCI Adult, German Credit, and Community & Crime datasets.

eliminated by rewriting these expectations as *w.r.t.* the data distribution. For example, we can rewrite $\langle \lambda_{S_a}(s) \rangle_{p_{S_a}(s)}$ as

$$\langle \lambda_{S_a}(s) \rangle_{p_{S_a}(s)} = \langle \lambda_{S_a}(g_\theta(a, x)) \rangle_{p(x|a)},$$

and then make a Monte-Carlo approximation using $\{s_a^i = g_\theta(a, x^i)\}_{i=1}^{N_S}$. Indeed, using the change of variables rule for $s = g_\theta(a, x)$ and $p_{S_a}(s)|\partial s/\partial x| = p(x|a)$, we can write

$$\begin{aligned} \langle \lambda_{S_a}(s) \rangle_{p_{S_a}(s)} &= \int_x p_{S_a}(g_\theta(a, x)) \lambda_{S_a}(g_\theta(a, x)) |\partial s/\partial x| \\ &= \int_x p(x|a) \lambda_{S_a}(g_\theta(a, x)). \end{aligned}$$

Using the chain rule, we obtain the stochastic-gradient update³

$$\begin{aligned} \theta \leftarrow \theta - \epsilon_\theta \sum_{a \in \mathcal{A}} \sum_{i=1}^{N_S} \sum_{j=1}^{N_S} &\left((1 - \alpha_{ij}) \nabla_{g_\theta} \lambda_{S_a}(s_a^i) \right. \\ &\left. + \alpha_{ij} \nabla_{g_\theta} \mathcal{C}(s_a^i, \bar{s}^j) \right) \nabla_{\theta} s_a^i, \end{aligned}$$

with $\nabla_{g_\theta} \lambda_{S_a}(s_a^i) = -\sqrt{\frac{2}{D}} \lambda_{S_a}^\top(\omega^1 s_a^i + b^1), \dots, \omega^D \sin(\omega^D s_a^i + b^D)$, $\nabla_{g_\theta} \mathcal{C}(s_a^i, \bar{s}^j) = \text{sign}(s_a^i - \bar{s}^j)$, and $\nabla_{\theta} s_a^i = (a, x^i)^\top s_a^i (1 - s_a^i)$.

Results

We first compare the COT method with two discrete OT methods introduced in Jiang et al. (2019) in the standard static fairness scenario. We show superior performance of COT when little data is available to solve the OT problem, and similar performance otherwise. We then consider a scenario in which the unfairness level is assumed to change, and show that OT methods are able to continually adjust the model parameters to adapt to such changes.

The first method introduced in Jiang et al. (2019) (referred to as *DOT*) can be seen as the discrete counterpart of COT. More specifically, DOT alternates between the following two steps:

1. Estimate the optimal coupling matrix as

$$T_a^* = \arg \min_T \langle T, \mathcal{C} \rangle, \quad (8)$$

for $T \in \mathbb{R}^{N_S \times N_S}$ s.t. $T \mathbf{1}_{\bar{S}} = \frac{1}{N_S} \mathbf{1}_{N_S}$ and $T^\top \mathbf{1}_S = \frac{1}{N_S} \mathbf{1}_{\bar{S}}$, where $\mathbf{1}_{N_S}$ denotes a vector of ones of size N_S .

³With the term $\frac{1}{N_S N_S}$ absorbed into ϵ_θ .

2. Perform a gradient update of the model parameters θ as

$$\theta \leftarrow \theta - \epsilon_\theta \sum_{a \in \mathcal{A}} \sum_{i=1}^{N_S} \sum_{j=1}^{N_S} T_a^*(i, j) \nabla_{g_\theta} \mathcal{C}(s_a^i, \bar{s}^j) \nabla_{\theta} s_a^i.$$

When \mathcal{C} is an L^p cost, it can be shown that T_a^* is sparse. In this case the computational cost is $\mathcal{O}(N_S + N_{\bar{S}})$.

The second method introduced in Jiang et al. (2019) (referred to as *DPP*) is an approximate quantile post-processing method to match the model outputs to $p_{\bar{S}}$.

The logistic regression (*LR*) parameters θ^* used to initialize COT, DOT, and DPP were obtained using scikit-learn with default hyper-parameters (Pedregosa and et al. 2011). The number of gradient updates for COT and DOT was set to $K = 100,000$. An ablation study on the Adult dataset showed that COT gives similar performance for number of random Fourier features $D \geq 50$, for kernel variance in the range $\sigma^2 = \{.01, .1, 1\}$, and for the entropy and L^2 regularizations. We only considered the summation for $i = j$ by imposing $N_S = N_{\bar{S}}$, which reduces the computation cost. Both COT and DOT required careful selection of the gradient update size ϵ_θ . In addition, COT required careful tuning of ϵ_θ with the dual variables update size ϵ_λ and regularization strength λ . COT tended to display some instability during training, which could in some cases be alleviated with the constraint $\lambda_X(x) + \lambda_Y(x) = 0$.

Fixed Level of Unfairness

We compared LR, DOT, DPP, and COT on the following datasets from the UCI repository (Lichman 2013):

Adult Dataset. This dataset contains 14 attributes for 48,842 individuals. The class label corresponds to annual income (below/above \$50,000). As sensitive attributes we considered race (Black and White) and gender (female and male), obtaining four groups.

German Credit Dataset. This dataset contains 20 attributes for 1,000 individuals applying for loans. Each applicant is classified as a good or bad credit risk, *i.e.* as likely or not likely to repay the loan. As sensitive attributes we considered age (below/equal or above 30 years old), obtaining two groups.

Communities & Crime Dataset. This dataset contains 135 attributes for 1994 communities. The class label corresponds to crime rate (below/above the 70-th percentile). As sensitive attributes we considered race (Black, White, Asian, and Hispanic) thresholded at the median, obtaining height groups.

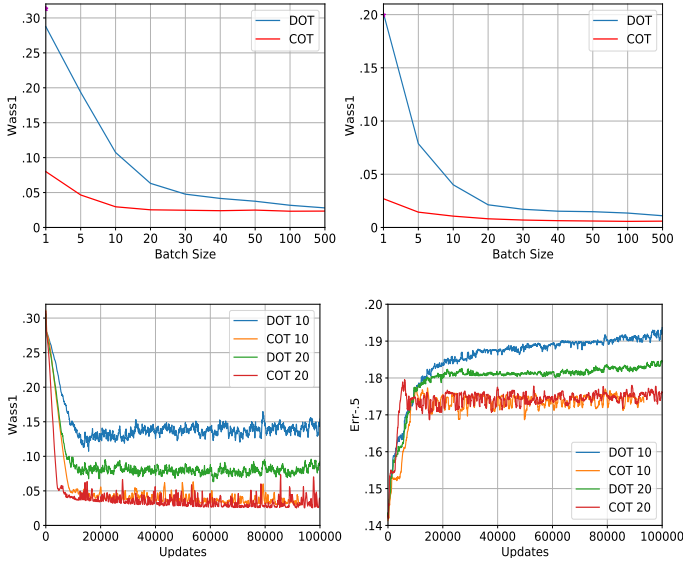


Figure 2: **Top Left:** W1 for DOT and COT on the Adult dataset using different batch sizes. The magenta star indicates W1 for LR. **Bottom:** Evolution of W1 and Err-.5 for batch sizes 10 and 20 over the 100,000 gradient updates. **Top Right:** The same as Top Left but considering only gender as sensitive attribute and the male outputs distribution as target distribution.

We used the Wasserstein-1 barycenter as target distribution $p_{\bar{S}}$ and the following metrics:

Err-.5: Classification error at $\tau = 0.5 \frac{1}{N} \sum_{n=1}^N \mathbb{1}_{\hat{y}^n \neq y^n}$,

W1: Wasserstein-1 distance $\sum_{a \in \mathcal{A}} \mathcal{W}_1(p_{S_a}, p_{\bar{S}})$,

SDD: Strong Demographic Disparity $\sum_{a \in \mathcal{A}} \mathbb{E}_{\tau \sim U([0,1])} |\mathbb{P}(S_a > \tau) - \mathbb{P}(S > \tau)|$,

SPDD: Strong Pairwise Demographic Disparity $\frac{1}{2} \sum_{a, \bar{a} \in \mathcal{A}} \mathbb{E}_{\tau \sim U([0,1])} |\mathbb{P}(S_a > \tau) - \mathbb{P}(S_{\bar{a}} > \tau)|$,

computed as in Jiang et al. (2019).

Test results are given in Table 1. We can see that the OT methods generally perform similarly, except for the German Credit dataset in which DOT has higher error for similar unfairness level.

Solving the OT Problem with Limited Data. In real-world applications, the amount of data available to solve the OT problem might be limited—this could be the case, *e.g.*, if data needs to be disregarded due to privacy issues.

As the number of samples tends to infinity, the DOT Wasserstein-1 distance (and corresponding gradient) estimator approaches the true distance. Nevertheless, if the batch size is small, the resulting (random) estimator is biased as its expectation would not correspond to the true distance. For COT, we rely on the fact that it is possible to compute unbiased gradient estimators of the regularized Wasserstein-1 distance. This means that, using these estimators, it is possible to reach an arbitrarily (up to the batches variance) good

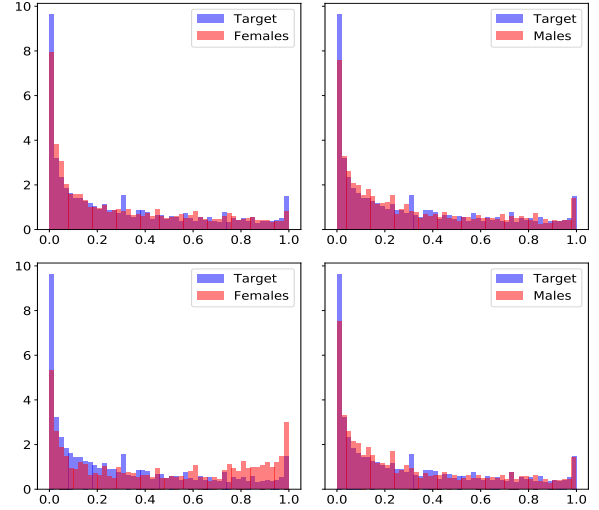


Figure 3: Effect of change in unfairness level on COT on the Adult dataset, considering gender as sensitive attribute and the male outputs distribution as target distribution. **Top:** Histograms of the target distribution, and of the female and male outputs distributions produced by a model constrained to achieve SDP on a subset of the dataset with .1 and .3 probability of belonging to class 1 for female and male individuals respectively. **Bottom:** Histograms produced by the same model, but using a subset of the dataset with .4 probability that a female individual belongs to class 1.

estimator of the regularized Wasserstein-1 distance by sampling sufficiently many random batches. Nevertheless, this estimator will always be a biased version of the true distance, as it will converge to its regularized counterpart.

To empirically test the effect of bias when little data is available, we compared COT and DOT on the Adult dataset with varying batch sizes $N_S = N_{\bar{S}}$. As we can see in Fig. 2(Top Left), for smaller batch sizes DOT has higher W1 than COT (the W1 value for LR is indicated with a magenta star). As we can see from the W1 and Err-.5 evolution over the 100,000 gradient updates for batch sizes 10 and 20 in Fig. 2(Bottom), DOT has higher error than COT despite higher W1. This suggests that the estimates of the optimal coupling matrix T_a^* (Eq. (8)) are inaccurate, as if the issue were *e.g.* with penalization or with a suboptimal choice of ϵ_θ higher W1 would correspond to smaller error. Fig. 2(Top Right) shows that the same qualitative conclusions also hold for the simpler case of considering only gender as sensitive attribute and the male outputs distribution as target distribution.

Changing Level of Unfairness

In real-world applications, the data on which a system is deployed might contain a different level of unfairness than the data on which the system was enforced to be fair. This could be the case, *e.g.*, for a risk assessment instrument deployed in a geographic area where over-policing in certain neighborhoods occurs at different rates than in the data used to

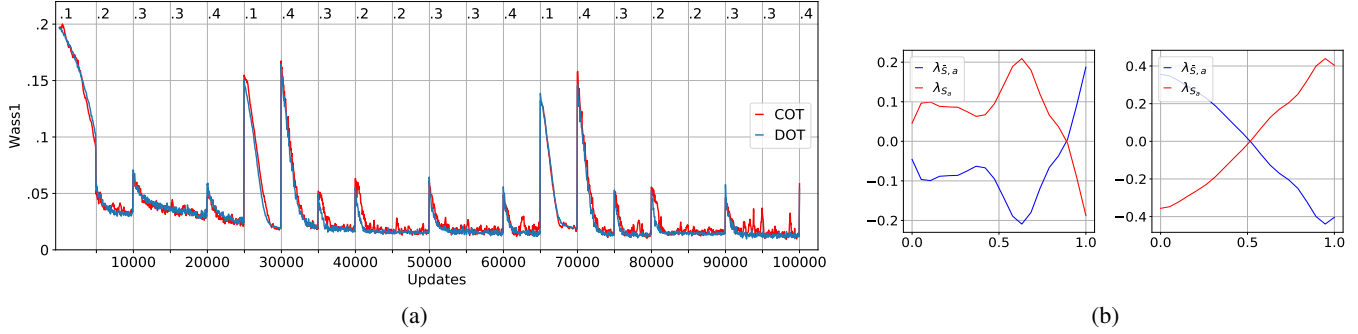


Figure 4: **(a):** Wass1 for COT and DOT over 100,000 gradient updates, with changing (every 5,000 updates) probability of belonging to class 1 for female individuals as indicated at the top. **(b):** Dual variables for female individuals shortly before and after 30,000 updates in (a).

train the system. Or for a system deployed later in the future, when biases have changed, *e.g.* as a consequence of the decisions taken by the system.

In Fig. 3, we illustrate the effect of change in unfairness level on COT on the Adult dataset, considering gender as sensitive attribute and the male outputs distribution as target distribution. In the Adult dataset, the probability that a female individual belongs to class 1 (has annual income above \$50,000) is .1, as opposed to .3 for a male individual. Fig. 3(Top) shows histograms of the target distribution, p_S (blue), and of the female and male outputs distributions, p_{S_a} (red), produced by a model that was constrained to achieve SDP on a subset of the dataset with the same probabilities of belonging to class 1. Fig. 3(Bottom) shows histograms produced by the same model, but using a subset of the dataset in which the probability of belonging to class 1 is .4 for female individuals and .3 for male individuals. Due to the increase of probability from .1 to .4, the model gives a distribution of female outputs that has too much mass toward higher probability of belonging to class 1.

The underlying assumption when using SDP as fairness criterion is that existing dependencies between A and X , and between A and Y are unfair (and therefore should not be encoded in the model output S). Therefore, a different relationship between A and X through a conditional distribution $p_t(X|A)$ that differs from the original distribution $p(X|A)$ would result in a different unfairness level. A dataset \mathcal{D}_t with underlying joint distribution $p_t(A, X, Y) = p(Y|A, X)p_t(X|A)p(A)$ can indirectly be obtained by sampling a subset of the original dataset \mathcal{D} with a different probability of belonging to class 1, $p_t(Y = 1|A)$.

We created a sequence of such datasets, $\{\mathcal{D}_t\}$, by sampling subsets of the Adult dataset in which female individuals had the following probabilities of belonging to class 1: .2, .3, .3, .4, .1, .4, .3, .2, .2, .3, .3, .4, .1, .4, .3, .2, .2, .3, .3, .4. We trained COT and DOT for a total of 100,000 gradient updates starting from $\mathcal{D}_1 \equiv \mathcal{D}$ and then moving to the next dataset in the sequence every 5,000 updates.

The resulting Wass1 is shown in Fig. 4(a) (values are plotted every 50 updates). Both COT and DOT adapt well to

changes in unfairness levels and behave very similarly, although DOT is more stable. Interestingly, earlier in the training Wass1 is higher than later in the training when the probability of belonging to class 1 is also .1, and requires more updates to reach a low value. This indicates that, after the first modifications of the LR parameters θ^* , θ reach a region of the space that enables fast adjustment. The fact that the minimum value of Wass1 decreases with progressing in the gradient updates also indicates that both COT and DOT modify the parameters in a way that is independent of the specific unfairness level contained in the dataset. Whilst on the Adult dataset it takes more than 50,000 updates for Wass1 to reach minimum levels given the logistic regression (LR) initialization, the right part of Fig. 4(a) shows that, on a subset of the dataset with the same probabilities of belonging to class 1, it does not take that many updates given an initialization at the model that was already adjusted for a different level of unfairness. Together with the left part, Fig. 4(a) shows that the parameters move to an area of the space that allows to quickly reach lower and lower Wass1. Overall these experiments show that OT can quickly adjust to changes in the underlying unfairness level and without the need of retraining the model from scratch.

In Fig. 4(b), we show the dual variables for the female group shortly before and after gradient update 30,000 of Fig. 4(a). As we can see, before update 30,000 the values of λ_{S_a} and λ_{S_s} are small and close to each-other over the interval $[0, 1]$, indicating that the female and target distributions are similar. After update 30,000 the values are higher and differ mostly at the extremes of the interval $[0, 1]$, indicating that the female and target distributions differ the most in this parts of the space. These two plots corresponds to the first histograms in Fig. 3(Top) and Fig. 3(Bottom) respectively.

Conclusions

We have proposed a stochastic-gradient fairness method based on a dual formulation of continuous OT that displays superior performance to discrete OT methods when little data is available to solve the OT problem, and similar performance otherwise. In addition, we have shown that both

continuous and discrete OT methods are suitable to continual adjustments of the model parameters to adapt to changes in levels of unfairness that might occur in real-world applications of ML systems.

References

- Arjovsky, M.; Chintala, S.; and Bottou, L. 2017. Wasserstein Generative Adversarial Networks. In *Proceedings of the 34th International Conference on Machine Learning*, 214–223.
- Barocas, S.; Hardt, M.; and Narayanan, A. 2019. *Fairness and Machine Learning*. fairmlbook.org.
- Black, E.; S., Y.; and Fredrikson, M. 2019. FlipTest: Fairness Auditing via Optimal Transport. *CoRR* abs/1906.09218.
- Blum, A.; Gunasekar, S.; Lykouris, T.; and Srebro, N. 2018. On Preserving Non-discrimination when Combining Expert Advice. In *Advances in Neural Information Processing Systems 31*, 8376–8387.
- Celis, L. E.; and Vijay Keswani, V. 2019. Improved Adversarial Learning for Fair Classification. *CoRR* abs/1901.10443.
- Chiappa, S.; Jiang, R.; Stepleton, T.; Pacchiano, A.; Jiang, H.; and Aslanides, J. 2020. A General Approach to Fairness with Optimal Transport. In *Thirty-Fourth AAAI Conference on Artificial Intelligence*, 3633–3640.
- Chzhen, E.; Denis, C.; Hebiri, M.; Oneto, L.; and Pontil, M. 2020. Fair Regression with Wasserstein Barycenters. In *Advances Neural Information Processing Systems 33*.
- Creager, E.; Madras, D.; Pitassi, T.; and Zemel, R. 2019. Causal Modeling for Fairness in Dynamical Systems. *CoRR* abs/1909.09141.
- Csiszar, I. 1975. I -Divergence Geometry of Probability Distributions and Minimization Problems. *Annals of Probability* 3(1): 146–158.
- Del Barrio, E.; Gamboa, F.; Gordaliza, P.; and Loubes, J.-M. 2019. Obtaining Fairness Using Optimal Transport Theory. In *Proceedings of the 36th International Conference on Machine Learning*, 2357–2365.
- Del Barrio, E.; Gordaliza, P.; and Loubes, J. 2020. Review of Mathematical Frameworks for Fairness in Machine Learning. *CoRR* abs/2005.13755.
- Gajane, P.; and Pechenizkiy, M. 2017. On formalizing fairness in prediction with machine learning. *CoRR* abs/1710.03184.
- Genevay, A. 2019. *Entropy-regularized Optimal Transport for Machine Learning*. Ph.D. thesis, PSL Research University.
- Genevay, A.; Cuturi, M.; Peyré, G.; and Bach, F. 2016. Stochastic Optimization for Large-scale Optimal Transport. In *Advances in Neural Information Processing Systems 29*, 3440–3448.
- Gillen, S.; Jung, C.; Kearns, M.; and Roth, A. 2018. Online Learning with an Unknown Fairness Metric. In *Advances in Neural Information Processing Systems 31*, 2600–2609.
- Jabbari, S.; Joseph, M.; Kearns, M.; Morgenstern, J.; and Roth, A. 2017. Fairness in Reinforcement Learning. In *Proceedings of the 34th International Conference on Machine Learning*, 1617–1626.
- Jiang, R.; Pacchiano, A.; Stepleton, T.; Jiang, H.; and Chiappa, S. 2019. Wasserstein Fair Classification. In *Thirty-Fifth Uncertainty in Artificial Intelligence Conference*.
- Johnrow, J. E.; and Lum, K. 2019. An Algorithm for Removing Sensitive Information: Application to Race-independent Recidivism Prediction. *The Annals of Applied Statistics* 13(1): 189–220.
- Joseph, M.; Kearns, M.; Morgenstern, J. H.; and Roth, A. 2016. Fairness in Learning: Classic and Contextual Bandits. In *Advances in Neural Information Processing Systems 29*, 325–333.
- Kantorovich, L. 1942. *On the Transfer of Masses (in Russian)*. Doklady Akademii Nauk.
- Le Gouic, T.; and Loubes, J.-M. 2020. The Price for Fairness in a Regression Framework. *CoRR* abs/2005.11720.
- Lee, J.; Pacchiano, A.; and Jordan, M. 2020. Convergence Rates of Smooth Message Passing with Rounding in Entropy-regularized MAP Inference. In *Twenty-Third International Conference on Artificial Intelligence and Statistics*, 3003–3014.
- Lichman, M. 2013. UCI Machine Learning Repository. URL <http://archive.ics.uci.edu/ml>.
- Liu, L.; Dean, S.; Rolf, E.; Simchowitz, M.; and Hardt, M. 2018. Delayed Impact of Fair Machine Learning. In *Proceedings of the 35th International Conference on Machine Learning*, 3150–3158.
- Lum, K.; and Isaac, W. S. 2016. To predict and serve? *Significance* 13(5): 14–19.
- Mandal, D.; Deng, S.; Jana, S.; Wing, J. M.; and Hsu, D. J. 2020. Ensuring Fairness Beyond the Training Data. In *Advances in Neural Information Processing Systems 33*.
- Mensch, A.; and Peyré, G. 2020. Online Sinkhorn: Optimal Transport Distances from Sample Streams. *CoRR* abs/2003.01415.
- Mitchell, S.; Potash, E.; and Barocas, S. 2018. Prediction-based Decisions and Fairness: A Catalogue of Choices, Assumptions, and Definitions. *CoRR* abs/1811.07867.
- Oneto, L.; and Chiappa, S. 2020. Fairness in Machine Learning. In Oneto, L.; Navarin, N.; Sperduti, A.; and Anguita, D., eds., *Recent Trends in Learning From Data. Studies in Computational Intelligence*, volume 896. Springer, Cham.
- Pedregosa, F.; and et al. 2011. Scikit-learn: Machine Learning in Python. *Journal of Machine Learning Research* 12: 2825–2830.
- Peyré, G. and M. Cuturi, M. 2019. Computational Optimal Transport. *Foundations and Trends in Machine Learning* 11(5-6): 355–607.

- Rahimi, A.; and Recht, B. 2008. Random Features for Large-scale Kernel Machines. In *Advances in Neural Information Processing Systems 20*, 1177–1184.
- Risser, L.; Vincenot, Q.; Couellan, N.; and Loubes, J.-M. 2019. Using Wasserstein-2 Regularization to Ensure Fair Decisions with Neural-network Classifiers. *CoRR* abs/1908.05783.
- Rosenberg, M.; and Levinson, R. 2018. Trump’s Catch-and-detain Policy Snares Many Who Call the U.S. Home. URL <https://www.reuters.com/investigates/special-report/usa-immigration-court>.
- Seguy, V.; Damodaran, B. B.; Flamary, R.; Courty, N.; Rolet, A.; and Blondel, M. 2018. Large-Scale Optimal Transport and Mapping Estimation. In *7th International Conference on Learning Representations*.
- Sun, Y.; Ramirez, I.; Cuesta-Infante, A.; and Veeramachaneni, K. 2019. Learning Fair Classifiers in Online Stochastic Settings. *CoRR* abs/1908.07009.
- Tabibian, B.; Gómez, V.; De, A.; Schölkopf, B.; and Rodriguez, M. 2019. Consequential Ranking Algorithms and Long-term Welfare. *CoRR* abs/1905.05305.
- Verma, S.; and Rubin, J. 2018. Fairness Definitions Explained. In *IEEE/ACM International Workshop on Software Fairness*.
- Villani, C. 2009. *Optimal Transport Old and New*. Springer.
- Wang, H.; Ustun, B.; and Calmon, F. 2019. Repairing without Retraining: Avoiding Disparate Impact with Counterfactual Distributions. In *Proceedings of the 36th International Conference on Machine Learning*, 6618–6627.
- Wen, M.; Bastani, O.; and Topcu, U. 2019. Fairness with Dynamics. *CoRR* abs/1901.08568.
- Yurochkin, M.; Bower, A.; and Sun, Y. 2020. Training Individually Fair ML Models with Sensitive Subspace Robustness. In *9th International Conference on Learning Representations*.
- Zhang, B. H.; Lemoine, B.; and Mitchell, M. 2018. Mitigating Unwanted Biases with Adversarial Learning. In *Proceedings of the 2018 AAAI/ACM Conference on AI, Ethics, and Society*, 335–340.
- Zhang, X.; and Liu, M. 2020. Fairness in Learning-based Sequential Decision Algorithms: A Survey. *CoRR* abs/2001.04861.